Pharmacology, Biochemistry and Behavior 100 (2012) 361–369

Contents lists available at SciVerse ScienceDirect

Pharmacology, Biochemistry and Behavior

journal homepage: www.elsevier.com/locate/pharmbiochembeh

S14G-Humanin improves cognitive deficits and reduces amyloid pathology in the middle-aged APPswe/PS1dE9 mice

Wenjun Zhang [a,1], Wei Zhang [b,1], Zhuyi Li [a,b,1], Jian Hao [a], Zhuo Zhang [a,b], Liu Liu [a,b], Ni Mao [a], Jianting Miao [a,*], Lianfeng Zhang [c,**]

[a] Department of Neurology, Tangdu Hospital, Fourth Military Medical University, Xi'an City, Shaanxi Province 710038, China
[b] Institute of Functional Brain Disorders, Tangdu Hospital, Fourth Military Medical University, Xi'an City, Shaanxi Province 710038, China
[c] Institute of Laboratory Animal Science, Chinese Academy of Medical Sciences, Beijing City 100021, China

ARTICLE INFO

Article history:
Received 26 June 2011
Received in revised form 21 September 2011
Accepted 24 September 2011
Available online 2 October 2011

Keywords:
Alzheimer's disease
Amyloid-beta protein
S14G-Humanin
Cognitive deficits
Inflammation
Transgenic mice

ABSTRACT

Alzheimer's disease (AD) is a progressive neurodegenerative disorder characterized by clinical cognitive decline and pathological deposition of amyloid-beta protein (Aβ) in the brain. So far, there has been no causative therapy for this devastating disease. S14G-Humanin (HNG), a synthetic derivative of Humanin (HN), has been shown to have strong neuroprotective ability against AD-related insults in vitro and prevent cognitive impairments in Aβ-infused animal models. In addition, a recent study has reported a beneficial effect of intranasal HNG treatment on memory deficit and Aβ accumulation in triple transgenic (3xTg-AD) mice at the early plaque-bearing stage. However, whether HNG treatment has the disease-modifying efficacy on AD with pre-existing well-established amyloid plaque pathology remains unclear. In this study, we employed 9-month-old APPswe/PS1dE9 mice with pre-existing robust amyloid plaque pathology to investigate the effects of chronic HNG treatment on the progression of cognitive dysfunction and Aβ-associated neuropathology. We found that vehicle-treated APPswe/PS1dE9 mice showed impaired spatial learning and memory compared with vehicle- and HNG-treated wild-type mice, while intraperitoneal HNG treatment for 3 months significantly improved spatial learning and memory deficits in APPswe/PS1dE9 mice compared with vehicle control treatment. Coincidental with this, HNG treatment significantly reduced cerebral Aβ plaque deposition, insoluble Aβ levels, and neuroinflammatory responses in APPswe/PS1dE9 mice compared with control treatment. Cumulatively, these findings demonstrate that chronic administration of HNG is able to attenuate cognitive deficits and reduce Aβ loads as well as neuroinflammation in the middle-aged APPswe/PS1dE9 mice even with pre-existing substantial Aβ neuropathology, indicating that HNG has potential as a pharmacotherapeutic intervention in the development of cognitive deficits and neuropathology seen in the cases of established AD.
© 2011 Elsevier Inc. All rights reserved.

1. Introduction

Alzheimer's disease (AD) is a common neurodegenerative disorder that causes dementia in the elderly population worldwide, characterized clinically by cognitive impairments that progress to dementia (St George-Hyslop and Petit, 2005). Although the exact etiology of AD has not been clarified completely, increasing evidence has shown that overproduction of amyloid-beta (Aβ) protein, derived from the amyloid precursor protein (APP) by proteolytic cleavage at the β- and γ-secretase sites, and its accumulation in brain contribute to the underlying pathogenesis of AD for the progressive development of the disease (Selkoe, 1994; Selkoe, 2001; St George-Hyslop and Petit, 2005).

The acetylcholinesterase inhibitors (i.e., donepizil, rivastigmine, galantamine) and the N-methyl-D-aspartate (NMDA) receptor antagonist (memantine) have been developed and currently approved for treating patients with AD (Lleó et al., 2006; Seltzer, 2006; Smith et al., 2006). Although many clinical trials show that these drugs produce modest symptomatic benefit for improving cognitive deficits associated with the disease respectively, they have limited effect on substantially delaying the onset or modifying the progression of the disease (Schenk, 2008; Van Marum, 2008; Cappell et al., 2010; Herrmann et al., 2011). Unfortunately, no causal therapeutic agent for this devastating disease has been established so far. Thus, given the disease's growing prevalence and its poor prognosis, there is an urgent need to develop the novel therapeutic approaches with alternative, more effective, therapies that not only target the disease symptoms

* Correspondence to: J. Miao, Department of Neurology, Tangdu Hospital, Fourth Military Medical University, Xi'an City, Shaanxi Province 710038, China. Tel.: +86 29 84778342; fax: +86 29 83552982.
** Correspondence to: L. Zhang, Institute of Laboratory Animal Science, Chinese Academy of Medical Sciences, Beijing City 100021, China. Tel.: +86 10 87778442; fax: +86 10 67761943.
E-mail addresses: jtmiao@fmmu.edu.cn (J. Miao), zhanglf@cnilas.org (L. Zhang).
[1] Zhang W, Zhang W, and Li Z contributed equally to this work.

0091-3057/$ – see front matter © 2011 Elsevier Inc. All rights reserved.
doi:10.1016/j.pbb.2011.09.012

but can also slow or halt the underlying neuropathological process (Cappell et al., 2010; Herrmann et al., 2011; O'Hare et al., 2010).

Humanin (HN) is a novel 24-amino acid peptide, originally identified from an occipital lobe of an AD patient (Hashimoto et al., 2001), which has been reported to be an effective neuroprotective agent against cytotoxicity by all sorts of AD-relevant insults in vitro (Hashimoto et al., 2001; Arakawa et al., 2008; Kunesová et al., 2008; Jin et al., 2010). Surprisingly, S14G-Humanin (HNG), a derivative of HN (substitution of Gly for Ser14 of HN), has been shown to enhance its neuroprotective activity to an extent about 1000-fold than HN, which is effective at low nanomolar concentrations against AD-relevant insults in vitro (Nishimoto et al., 2004; Niikura et al., 2006). In addition to the in vitro assays, several in vivo studies have been conducted to evaluate the effect of HN and its derivative on cognitive functions by using different behavioral tests. The first in vivo study described the effect of the HN-derivative HNG on cognitive impairment in the Y-maze test showed that intracerebroventricular administration of HNG could reverse the scopolamine-induced impairment of spontaneous alternation behavior in mice (Mamiya and Ukai, 2001). Subsequently, intraperitoneal administration of HNG has been demonstrated to be effective on 3-quinuclidinyl benzilate (a muscarinic acetylcholine receptor antagonist)-induced impairment of spatial memory in the multiple T-maze in rats (Krejcova et al., 2004). As reported later, Tajima and coworkers have shown that intracerebroventricular injection of HNG might prevent Aβ-induced impairment of short-term/spatial working memory in the Y-maze test and impairment of latent learning in the water-finding test (Tajima et al., 2005). We also previously demonstrated that intraperitoneal injection of HNG resulted in a significant effect on improving memory deficits in Aβ-infused mice (Miao et al., 2008). Recently, Niikura and coworkers found that intranasal HNG treatment for 3 months ameliorated cognitive dysfunction and reduced amyloid burden in triple transgenic (3xTg-AD) mice at the early plaque-bearing stage (Niikura et al., 2011). Overall, these findings suggest that HNG might have potential as an AD therapeutic.

In fact, cognitive deficits as well as Aβ plaque deposition and its associated neuropathology exist for years before/once AD is clinically diagnosed (Kemppainen et al., 2007; Blurton-Jones et al., 2009). Hence, treatments that improve cognition and modify the disease progression of AD with the presence of well-established plaque pathology are urgently needed (Blurton-Jones et al., 2009). Therefore, research into the efficacy of therapeutic candidates on AD with pre-existing cognitive deficits and neuropathology is of critical importance for the development of new therapeutic drugs against AD. Although abundant evidence suggests that HNG may have a therapeutic potential in the treatment of AD, to our knowledge, no studies have yet explored the therapeutic effect of HNG on AD with pre-existing well-established plaque pathology.

The APPswe/PS1dE9 mouse is a well-established double transgenic model of AD, which harbors the mutant human genes APPswe (Swedish mutations K594N/M595L) and presenilin-1 with the exon-9 deletion (PS1-dE9) under control of the mouse prion protein promoter, and shows many features characteristic of the disease (Savonenko et al., 2005; Garcia-Alloza et al., 2006; Ruan et al., 2009; Wang et al., 2009; Li and Liu, 2010). The APPswe/PS1dE9 mice exhibit an early appearance of amyloid plaques at the age of 4 months (Garcia-Alloza et al., 2006; Ruan et al., 2009), and develop age-dependent increased amyloid plaque deposition and cognitive deficits (Lalonde et al., 2005; Savonenko et al., 2005; Minkeviciene et al., 2008; O'Leary and Brown, 2009). Moreover, central to the requirements of the current study, the middle-aged APPswe/PS1dE9 mice that already show cognitive deficits and well-established Aβ-related neuropathology may serve as a particularly useful model to clarify the effect of therapeutic candidates on cognitive deficits and AD-like pathology under the complex physiological conditions (Savonenko et al., 2005; Garcia-Alloza et al., 2006; Ruan et al., 2009; O'Leary and Brown, 2009; Zhang et al., 2011). To determine whether chronic HNG treatment has the disease-modifying efficacy on AD with pre-existing well-established amyloid plaque pathology, in the present study we used 9-month-old APPswe/PS1dE9 mice to examine the effects of HNG on progressively developing cognitive deficits and Aβ-related neuropathology.

2. Materials and methods

2.1. Animals and treatment

The APPswe/PS1dE9 mice used in the present study were generated and identified to be homozygous by professionals of the Institute of Laboratory Animal Science, Chinese Academy of Medical Science (Beijing China), and were generously provided by Dr. Lianfeng Zhang (Institute of Laboratory Animal Science, Chinese Academy of Medical Science, Beijing China). All the transgenic mice were genotyped for the presence of the mutant genes by PCR amplification of genomic DNA extracted from tail clippings as previously described (Wang et al., 2009; Wang et al., 2010; Li and Liu, 2010). Female APPswe/PS1dE9 mice and their matched non-transgenic wild-type (WT) littermates were randomly assigned into the following four groups ($n = 8$, each group): HNG-treated APPswe/PS1dE9 mice, vehicle-treated APPswe/PS1dE9 mice, HNG-treated WT mice, and vehicle-treated WT mice. Each mouse with HNG treatment received HNG (Peptide International Inc., USA) dissolved in normal saline every other day by intraperitoneal injection (0.1 μg/0.5 ml in saline), while each mouse with vehicle treatment received equal volume of saline injection (0.5 ml) as control according to the same schedule. Treatment was started when the mice were 9 months old and was continued for 3 months. Intraperitoneal administration of HNG has been shown to reverse the spatial memory impairment induced by 3-quinuclidinyl benzilate in rats (Krejcova et al., 2004), ameliorate behavioral deficits in Aβ-infused mice (Miao et al., 2008), and improve neurological deficits and reduce infarct size in mice (Xu et al., 2006), indicating that a substantial portion of intraperitoneally administered HNG passes through the blood–brain barrier. The dose and duration of HNG in this study were chosen based on our previous study (Miao et al., 2008) and on a review of literature (Krejcova et al., 2004; Xu et al., 2006).

Mice were housed in transparent plastic cages (2 mice per cage) according to standard animal care protocols and maintained in a pathogen-free environment with free access to rodent chow and water. The animals were randomized for therapy trials and coded, and the operators and data analyzer remained double blinded to which treatment they received, until the code was broken at the completion of data collection. Animal body weights were measured at the beginning of the experiment and every week thereafter. After the last injection, all animals were subjected to behavioral testing.

Protocols were conducted according to the University Policies on the Use and Care of Animals and were approved by the Institutional Animal Experiment Committee of Fourth Military Medical University, China.

2.2. Morris water maze test

After the treatment for 3 months, the spatial learning and memory were evaluated by the Morris water maze test as described previously (Maurice et al., 2009; Zhang et al., 2011). The apparatus consisted of a circular water tank (120 cm in diameter and 50 cm high). The water was rendered opaque by the addition of nontoxic white paint and the water temperature was maintained at 23 ± 1 °C. The swimming pool was surrounded by a set of extra-maze spatial cues (i.e., racks, a door, a watch, and pictures) on the walls, which were kept in fixed positions in the testing room where the water maze was placed. All conditions in the testing room were constant throughout the experiments.

For the acquisition (hidden-platform) test, the hidden platform (10 cm in diameter) was kept constant in the middle of one certain quadrant and submerged 1 cm below the water surface (30 cm away from the side wall) throughout training. The mice were required to

find the hidden platform using spatial cues available in the testing room where all conditions were constant throughout the experiments. The mice were subjected to four trials per day for 6 consecutive days. In each of the four trials, the mice were gently released into the water by facing the tank wall at four different starting positions equally spaced around the perimeter of the pool. They were given 60 s to find the submerged platform. On reaching the platform, the mice were allowed to stay on it for 20 s. If a mouse failed to locate the platform within 60 s, it was guided to the hidden platform and allowed to rest on it for 20 s, and a maximum score of 60 s was assigned. The time that an individual mouse took to reach the hidden platform was recorded as the escape latency (seconds) for its spatial learning score.

To assess the retention of spatial memory, a probe trial was performed 24 h after the last training trial. In this trial, the platform was removed from the tank, and the mice were allowed to swim freely for 60 s. The time that an individual mouse spent in the target quadrant previously containing the platform was recorded as a measure of spatial memory.

To test the visual, motor, and motivation skills of the mice, the visible platform tests (4 trials per day for 2 days) were performed 24 h after the probe trial. In this trial, the visible platform was positioned 1 cm above the water surface. The time to reach the visible platform and swimming speed were recorded and analyzed.

Trajectories of all animals were monitored and achieved with a computerized tracking system (Hampton Visual Systems Image 2020, UK). All time measurements were performed by using a stopwatch by an experimenter blinded to which experimental group to which each animal belonged throughout testing.

2.3. Brain tissue preparation

After behavioral tests, all animals were deeply anesthetized with sodium pentobarbital (100 mg/kg intraperitoneally), and perfused transcardially with 100 ml of cold normal saline. Brains were removed and dissected through the midsagittal plane. One hemisphere was placed in 70% ethanol, followed by xylene treatment and embedding in paraffin for immunohistochemical and histological analyses. The entire hippocampus and cerebral cortex were separately dissected from the remaining hemibrain and immediately snap-frozen and stored at −80 °C. The entire frozen hippocampus and cerebral cortex tissues each animal were separately pulverized into a fine powder which was then weighed and divided into small separate aliquots stored at −80 °C to be used for the biochemical analyses.

2.4. Quantification of cerebral Aβ levels

The levels of soluble and insoluble Aβ in the hippocampus and cerebral cortex of HNG- and vehicle-treated APPswe/PS1dE9 mice were quantified according to the procedures as described previously (Imbimbo et al., 2010; Zhang et al., 2011). Briefly, the tissue samples were weighed and homogenized in 5 vol/weight of TBS (Tris HCl 50 mM pH7.6; NaCl 150 mM; EDTA 2 mM) containing a cocktail of protease inhibitors (Sigma-Aldrich, USA). Homogenate was aliquoted and stored at −80 °C. One aliquot of each sample was suspended in 2% sodium dodecyl sulfate (SDS) containing protease inhibitors and centrifuged at 100,000 *g* for 60 min at 4 °C. The supernatant fraction was collected to be used for the soluble Aβ ELISA assay. The remaining SDS-insoluble pellet was sonicated and dissolved in 70% formic acid, and centrifuged at 100,000 xg for 60 min. The supernatant was collected to be used for the insoluble Aβ ELISA assay. The soluble and insoluble Aβ levels in all samples were determined employing the commercially available human Aβ1-x ELISA kit (Immuno-Biological Laboratories Co., Ltd., Japan), and Aβ1-40 and Aβ1-42 ELISA kits (BioSource, USA) according to the manufacturer's instructions. Data obtained in brain homogenates were expressed as nanograms of per milligrams of total protein (ng/mg total protein). Analyses were always performed in duplicate and in a coded manner. Protein content of brain homogenates was determined by using the Bio-Rad protein dye assay reagent.

2.5. Determination of cerebral APP βCTF

To determine the effect of HNG on the β-secretase activity, the human APP βCTF (carboxy-terminal fragments of APP cleaved by β-secretase) level in the hippocampus and cerebral cortex of HNG- and vehicle-treated APPswe/PS1dE9 mice was detected as described previously (Edbauer et al., 2003; Yamakawa et al., 2010). The amount of βCTF in brain was quantitatively determined using a Human APP βCTF Assay kit (Immuno-Biological Laboratories Co., Ltd., Japan) according to the manufacturer's protocol. The final values of brain APP βCTF were expressed as picomoles per milligrams of total protein (pm/mg protein). Analyses were always performed in duplicate and in a coded fashion.

2.6. Immunohistochemistry and histology

Immunohistochemical and histological staining was performed as described previously (Miao et al., 2005; Miao et al., 2008). Briefly, sections were cut in the sagittal plane at 10 μm thickness and mounted on slides. Sections were deparaffinated and rehydrated. Antigen retrieval was performed by treatment with proteinase K (0.2 mg/ml) for 10 min at room temperature for Aβ and astrocyte staining, and by 10 mM sodium citrate solution (pH 9.0) for 30 min at 90 °C in a water bath for activated microglia staining. Sections for nonspecific binding were blocked by incubating in PBS containing 0.1% Triton X-100 and 2% bovine serum albumin (Sigma-Aldrich, USA) for 20 min at room temperature. The sections were incubated with the following primary antibodies overnight at 4 °C for immunohistochemical analysis: mouse monoclonal antibody (6E10) which recognizes residues 1–17 of human Aβ (1:200; Millipore, USA), mouse monoclonal antibody to glial fibrillary acidic protein (GFAP) for the detection of astrocytes (1:500; Millipore, USA), and rabbit anti-Iba1 monoclonal antibody for the detection of activated microglia (1:300; Wako Pure Chemical Industries, Ltd., Japan). Primary antibodies were detected with horseradish peroxidase-conjugated or alkaline phosphatase-conjugated secondary antibodies and visualized with either a stable diaminobenzidine solution (Vector Laboratories, USA) according to the manufacturer's recommendations. As a negative control, sections from the same group of animals were treated in the same manner, except for the primary antibody. Thioflavin S staining for fibrillar plaques was performed with 1% Thioflavin S (Sigma-Aldrich, USA), and the green fluorescence–stained plaques were visualized using fluorescence microscopy.

2.7. Quantification of amyloid plaque burden and inflammatory cells

Quantitative image analysis was performed using Image-Pro Plus imaging software (version 5.0, Media Cybernetics, Bethesda, MD, USA) as described previously (Mori et al., 2006; Ruan et al., 2009; Zhang et al., 2011). In brief, to quantify immunoreactivity and Thioflavin S staining, images were acquired from the series of adjacent sections stained for immunohistochemistry and histology by using Olympus microscope connected to a digital microscope camera. For all treatment groups, the percentage of the area occupied by 6E10-positive plaques, Thioflavin-S-positive plaques, GFAP-positive immunoreactivity, and Iba1-positive immunoreactivity in the entire hippocampus and cerebral cortex was calculated respectively. Mean values for each parameter were recorded from six equidistant sections through the hippocampal region (at 150 μm intervals) per animal in each group. The threshold of detection was held constant during analysis and all measurements were conducted in a blinded fashion.

2.8. Measurement of brain cytokine levels

Mouse brain cytokine levels were assessed as described previously (Fan et al., 2007; Miao et al., 2008). Briefly, cerebral cortex tissues of all mice were separately homogenized in 10 volumes of 50 mm Tris–HCl, 150 mm NaCl, pH 7.5, containing protease inhibitor mixture (Sigma-Aldrich, USA) at 4 °C. The samples were centrifuged at 14,000 xg for 50 min at 4 °C. The protein concentrations of the supernatants were determined using the BCA kit (Pierce Biotechnology, USA). The levels of interleukin-1beta (IL-1β), interleukin-6 (IL-6), and tumor necrosis factor alpha (TNFa) in the samples were determined using a mouse IL-1β immunoassay kit (R&D Systems Inc., USA), a mouse IL-6 immunoassay kit (R&D Systems Inc., USA) and a mouse TNFa immunoassay kit (R&D Systems Inc., USA) in strict accordance with the manufacturer's instructions.

2.9. Statistical analysis

All data were expressed as mean ± SEM. The group differences in escape latency and swimming speed in the Morris water maze training task were analyzed using two-way repeated-measures ANOVA analysis followed by post hoc Bonferroni's test for multiple comparisons (Minkeviciene et al., 2004; Zhang et al., 2006; Peng et al., 2010). Data on the probe trial and neuroinflammatory assays were analyzed using one-way ANOVA analysis followed by post hoc Tukey's test for multiple comparisons (Minkeviciene et al., 2004; Miao et al., 2008). Treatment differences in the histological and biochemical Aβ assays between vehicle- and HNG-treated APPswe/PS1dE9 mice were analyzed by Student's *t* test (Peng et al., 2010). All analyses were performed with SPSS statistical package (version 13.0 for Windows, SPSS Inc., USA). A value of $p<0.05$ was considered statistically significant.

3. Results

3.1. HNG treatment ameliorates the spatial learning and memory deficits in APPswe/PS1dE9 mice

Spatial learning was assessed in the hidden platform task in all mice. As shown in Fig. 1A, there was a significant overall group difference in escape latency among the four groups (group effect: $F(3,28)=10.46$, $p<0.001$; training day effect: $F(5,140)=206.07$, $p<0.001$; group × training day interaction: $F(15,140)=1.06$, $p>0.05$). Vehicle-treated APPswe/PS1dE9 mice had significantly longer escape latency relative to vehicle- and HNG-treated WT mice ($p<0.001$, respectively), indicating that spatial learning deficits occurred in vehicle-treated APPswe/PS1dE9 mice. Whereas, HNG treatment in APPswe/PS1dE9 mice resulted in a significant decrease in escape latency compared with vehicle-treated APPswe/PS1dE9 mice ($p<0.01$), suggesting that HNG was effective in attenuating spatial learning deficits in APPswe/PS1dE9 mice.

A probe trial was conducted to assess the spatial memory in all mice. As shown in Fig. 1B, there was a significant overall group difference in the time spent in the target quadrant among the four groups ($F(3,31)=18.21$, $p<0.001$). Vehicle-treated APPswe/PS1dE9 mice spent less time in the target quadrant relative to vehicle- and HNG-treated WT mice ($p<0.001$, respectively), indicating that spatial memory was impaired in vehicle-treated APPswe/PS1dE9 mice. However, HNG-treated APPswe/PS1dE9 mice spent more time in the target quadrant compared to the vehicle-treated APPswe/PS1dE9 mice ($p<0.001$), suggesting that HNG was effective in attenuating spatial memory deficits in APPswe/PS1dE9 mice.

There were no significant differences in the escape latency (Fig. 1A) and the time spent in the target quadrant (Fig. 1B) between vehicle- and HNG-treated WT mice ($p>0.05$), indicating that HNG itself did not directly affect the learning and memory functions in WT mice. In addition, there was no significant difference in swimming speed during the acquisition training between the four groups of mice (Fig. S1; $p>0.05$). Moreover, no significant differences in escape latency (Fig. S2A) and swimming speed (Fig. S2B) in the visible platform test were observed between the four groups of mice ($p>0.05$). These results indicate that there were no overt behavioral deficits (i.e., inability to swim, inability to see the platform, and lack of motivation), as a result of the HNG injection. Thus, the impaired cognitive function in vehicle-treated APPswe/PS1dE9 mice and the improved cognitive function in HNG-treated in APPswe/PS1dE9 mice could not be attributable to non-cognitive factors (motor, visual, and motivation abnormalities). These findings support the hypothesis that HNG treatment led to the improvement of cognitive deficits in APPswe/PS1dE9 mice may be due to the attenuation of Aβ-associated neuropathology.

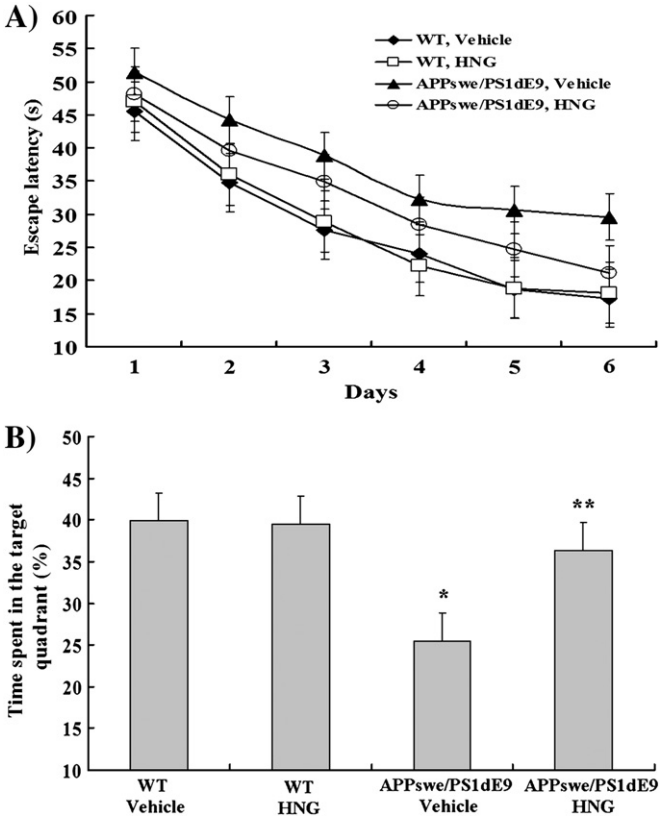

Fig. 1. HNG treatment improved spatial learning and memory deficits in APPswe/PS1dE9 mice. (A) Acquisition of spatial learning in the Morris water maze hidden platform task. Escape latency was used as a measure of spatial learning in the hidden platform task. Vehicle-treated APPswe/PS1dE9 mice had significantly longer escape latency compared with vehicle- and HNG-treated WT mice. HNG-treated APPswe/PS1dE9 mice had significantly lower escape latency compared with vehicle-treated APPswe/PS1dE9 mice. There was no significant difference in escape latency between vehicle- and HNG-treated WT mice ($p>0.05$). (B) Spatial memory test in the Morris water maze probe trial without platform. Vehicle-treated APPswe/PS1dE9 had significantly less time spent in the target quadrant relative to vehicle- and HNG-treated WT mice. HNG-treated APPswe/PS1dE9 mice had significantly more time spent in the target quadrant compared with vehicle-treated APPswe/PS1dE9 mice. There was no significant difference in the time spent in the target quadrant between vehicle- and HNG-treated WT mice ($p>0.05$). Each value represents the mean ± SEM from 8 mice per group. *$p<0.001$ versus vehicle- and HNG-treated WT mice; **$p<0.001$ versus vehicle-treated APPswe/PS1dE9 mice.

3.2. HNG treatment reduces cerebral plaque deposition in APPswe/PS1dE9 mice

The total Aβ plaques were detected by using a specific anti-Aβ antibody (6E10) and the fibrillar plaques by using Thioflavin S staining. Compared with vehicle-treated APPswe/PS1dE9 mice showing robust 6E10-positive and Thioflavin S-positive Aβ deposits in cerebral cortex and hippocampus (Fig. 2A and B), HNG-treated APPswe/PS1dE9 mice

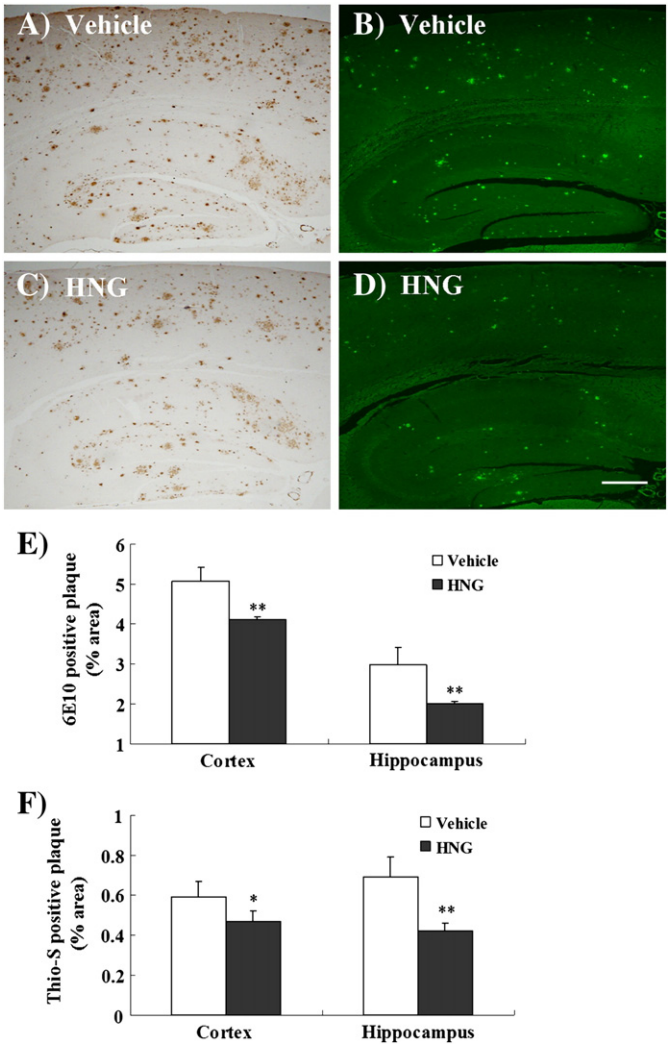

Fig. 2. HNG reduced Aβ deposition in APPswe/PS1dE9 mice. Amyloid plaques were stained with 6E10 antibody and Thioflavin S (ThioS) respectively. Vehicle-treated APPswe/PS1dE9 mice exhibited robust 6E10-positive plaques (A) and ThioS-positive fibrillar plaques (B) in the cerebral cortex and hippocampus, while HNG-treated APPswe/PS1dE9 mice showed a remarked decrease of both forms of the plaques (C and D). Quantification of amyloid plaques throughout the cerebral cortex and hippocampus revealed that HNG treatment led to a significant decrease in either total Aβ plaque burden (E) or fibrillar Aβ plaque burden (F) in APPswe/PS1dE9 mice. Each value represents the mean ± SEM from 8 mice per group. $^{*}p<0.01$, $^{**}p<0.001$ versus vehicle-treated APPswe/PS1dE9 mice. Scale bar = 200 μm.

exhibited a marked decrease in both forms of Aβ plaques (Fig. 2C and D). Quantitative analysis revealed that HNG treatment significantly reduced the total plaque load (Fig. 2E; $p<0.001$) and the fibrillar plaque load (Fig. 2F; $p<0.01$) in cerebral cortex and hippocampus of APPswe/PS1dE9 mice, indicating that HNG was effective in reducing the age-related increase of cerebral plaque burden in APPswe/PS1dE9 mice with pre-existing amyloid plaque pathology.

3.3. HNG treatment reduces insoluble Aβ levels in APPswe/PS1dE9 mice

The levels of soluble and insoluble Aβ in brain from APPswe/PS1dE9 mice treated with HNG or vehicle are shown in Fig. 3. Compared with vehicle controls, HNG treatment in APPswe/PS1dE9 mice significantly lowered the levels of insoluble total Aβ1-x (Fig. 3A; $p<0.001$), insoluble Aβ1-40 (Fig. 3C; $p<0.01$), and Aβ1-42 (Fig. 3E; $p<0.001$) in the cerebral cortex and hippocampus. However, there were no significant differences in the levels of soluble Aβ (total Aβ1-x, Aβ1-40, Aβ1-42) between the two groups (Fig. 3B, D, and F; $p>0.05$). These data confirm that HNG had some Aβ-lowering effect in APPswe/PS1dE9 mice.

3.4. HNG treatment has little effect on APP processing in APPswe/PS1dE9 mice

The level of APP βCTF was examined to determine whether HNG could influence APP processing. We found no significant difference in the APP βCTF levels in hippocampus and cerebral cortex between vehicle- and HNG-treated APPswe/PS1dE9 mice (Fig. 4; $p>0.05$). Together with the unchanged soluble Aβ levels in HNG-treated APPswe/PS1dE9 mice (Fig. 3B, D, and F), these results indicate that HNG treatment had little effect on the APP processing and Aβ generation.

3.5. HNG treatment reduces glial activation in APPswe/PS1dE9 mice

Immunohistochemical staining showed similar GFAP-positive astrocytes in vehicle-treated WT mice (Fig. 5A) and HNG-treated WT mice (Fig. 5B). In contrast, vehicle-treated APPswe/PS1dE9 mice showed markedly increased reactive astrocytes (Fig. 5C), while HNG-treated APPswe/PS1dE9 mice exhibited remarkably decreased reactive astrocytes (Fig. 5D). Quantitative analysis revealed that vehicle-treated APPswe/PS1dE9 mice had a significant increase in the amount of reactive astrocytes in cerebral cortex and hippocampus compared with vehicle- and HNG-treated WT mice (Fig. 5E; $p<0.001$, respectively), while HNG treatment in APPswe/PS1dE9 mice resulted in a significant decrease in the amount of reactive astrocytes in cerebral cortex and hippocampus compared with vehicle-treated APPswe/PS1dE9 mice (Fig. 5E; $p<0.01$).

Immunohistochemical staining showed fewer Iba1-positive microglia in vehicle-treated WT mice (Fig. 6A) and HNG-treated WT mice (Fig. 6B). In contrast, robust activated microglia was observed in vehicle-treated APPswe/PS1dE9 mice (Fig. 6C), while markedly decreased activated microglia was observed in HNG-treated APPswe/PS1dE9 mice (Fig. 6D). Quantitative analysis disclosed that vehicle-treated APPswe/PS1dE9 mice had a significant increase in the amount of activated microglia in cerebral cortex and hippocampus compared with vehicle- and HNG-treated WT mice (Fig. 6E; $p<0.001$, respectively), while HNG treatment in APPswe/PS1dE9 mice resulted in a significant decrease in the amount of activated microglia in cerebral cortex and hippocampus compared with vehicle-treated APPswe/PS1dE9 mice (Fig. 6E; $p<0.001$).

3.6. HNG treatment lowers the levels of inflammatory cytokines in APPswe/PS1dE9 mice

The levels of inflammatory cytokines in cerebral cortex were quantitatively measured by ELISA. As shown in Fig. 7, vehicle-treated APPswe/PS1dE9 mice had a significant increase in the levels of IL-1β (Fig. 7A; $p<0.001$), IL-6 (Fig. 7B; $p<0.01$), and TNFα (Fig. 7C; $p<0.001$) compared with vehicle- and HNG-treated WT mice, while HNG treatment in APPswe/PS1dE9 mice significantly reduced these elevated levels of IL-1β (Fig. 7A; $p<0.001$), IL-6 (Fig. 7B; $p<0.01$), and TNFα (Fig. 7C; $p<0.001$) compared with vehicle-treated APPswe/PS1dE9 mice.

4. Discussion

In the present study, we have demonstrated that that HNG treatment is effective in improving cognitive deficits and reducing cerebral Aβ deposition, insoluble Aβ levels, and neuroinflammation in the middle-aged APPswe/PS1dE9 mice with pre-existing abundant Aβ pathology.

Progressive cognitive decline is known to be a clinical hallmark of AD patients, and worsens with the disease progression, which imposes a large burden on patients and their families (Selkoe, 2001; St George-Hyslop and Petit, 2005). In this regard, the efficacy of any

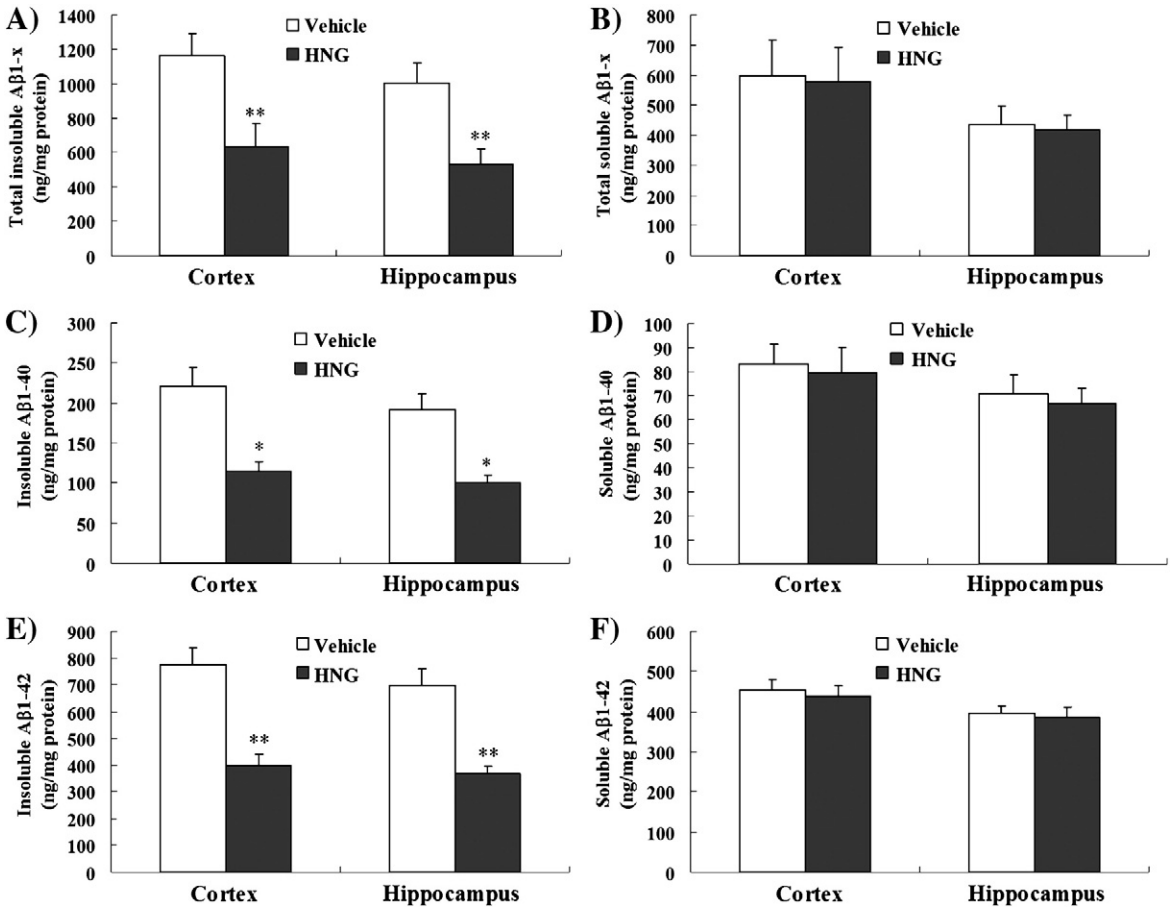

Fig. 3. HNG treatment reduced the levels of insoluble Aβ in APPswe/PS1dE9 mice. Levels of insoluble total Aβ1-x (A), Aβ1-40 (C), and Aβ1-42 (E) in cerebral cortex and hippocampus were significantly lower in HNG-treated APPswe/PS1dE9 mice than in vehicle-treated APPswe/PS1dE9 mice. There were no significant differences in levels of soluble total Aβ1-x (B), Aβ1-40 (D), and Aβ1-42 (F) in cerebral cortex and hippocampus between HNG- and vehicle-treated APPswe/PS1dE9 mice ($p>0.05$). Each value represents the mean ± SEM from 8 mice per group. $^{*}p<0.01$, $^{**}p<0.001$ versus vehicle-treated APPswe/PS1dE9 mice.

given intervention against AD would ultimately be judged upon its ability to prevent/improve cognitive decline. Previous studies have shown that APPswe/PS1dE9 mice exhibit spatial learning and memory impairments on the Morris water maze at 8 months of age (Lalonde et al., 2005; Butovsky et al., 2006; Oksman et al., 2006; Minkeviciene et al., 2008) and progressive cognitive deterioration as they age and pathology progresses (Savonenko et al., 2005; Minkeviciene et al., 2008; O'Leary and Brown, 2009). Hence, at the start of treatment at 9 months of age, these transgenic animals show significant deficits in learning and memory compared to non-transgenic animals. Behavioral analyses of the present study revealed that vehicle-treated APPswe/PS1dE9 mice already had spatial learning and memory deficits compared with WT mice, while HNG treatment significantly improved the cognitive deficits in APPswe/PS1dE9 mice. Importantly, HNG treatment in APPswe/PS1dE9 mice restored their spatial memory function to reach the level of WT mice. These data indicate an effective role of HNG in improving Aβ-related cognitive deterioration, which is consistent with the previous studies showing that intracerebroventricular or intraperitoneal injection of HNG may prevent Aβ-induced behavioral deficits in Aβ-infused mice (Tajima et al., 2005; Miao et al., 2008), and intranasal treatment of HNG can ameliorate cognitive impairment in 3xTg-AD male mice (Niikura et al., 2011). Together, these observations indicate that HNG treatment has a substantial effect on improving cognitive deficits associated Aβ.

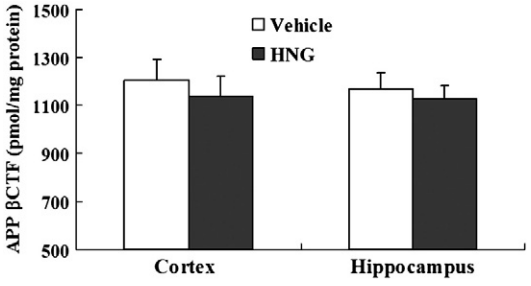

Fig. 4. HNG treatment had little effect on APP processing in APPswe/PS1dE9 mice. No significant differences in the APP βCTF level were found in cerebral cortex and hippocampus between HNG- and vehicle-treated APPswe/PS1dE9 mice ($p>0.05$). Each value represents the mean ± SEM from 8 mice per group.

Although the exact etiology of AD is not fully understood, substantial evidence has shown that Aβ peptide is central for the pathogenesis of AD (Selkoe, 2001; Hardy and Selkoe, 2002). Cerebral parenchymal Aβ deposition is a prominent pathological hallmark of AD, and can occur as diffuse or fibrillar plaques, with the latter associated with neurotoxicity (Selkoe, 2001; St George-Hyslop and Petit, 2005). Progressive Aβ production and its deposition over time have been shown in this transgenic model (Garcia-Alloza et al., 2006; Ruan et al., 2009). Consistent with the previous findings (Garcia-Alloza et al., 2006; Ruan et al., 2009), vehicle-treated APPswe/PS1dE9 mice exhibited abundant amyloid deposits in the brain, whereas HNG treatment in APPswe/PS1dE9 mice led to a significant reduction in total plaque burden (plaques stained with 6E10 antibody) and fibrillar plaque burden (plaques stained with thioflavine-S) in cerebral cortex and hippocampus compared with vehicle-treated APPswe/PS1dE9 mice. The beneficial effect of HNG on reducing Aβ deposition in brain was further confirmed

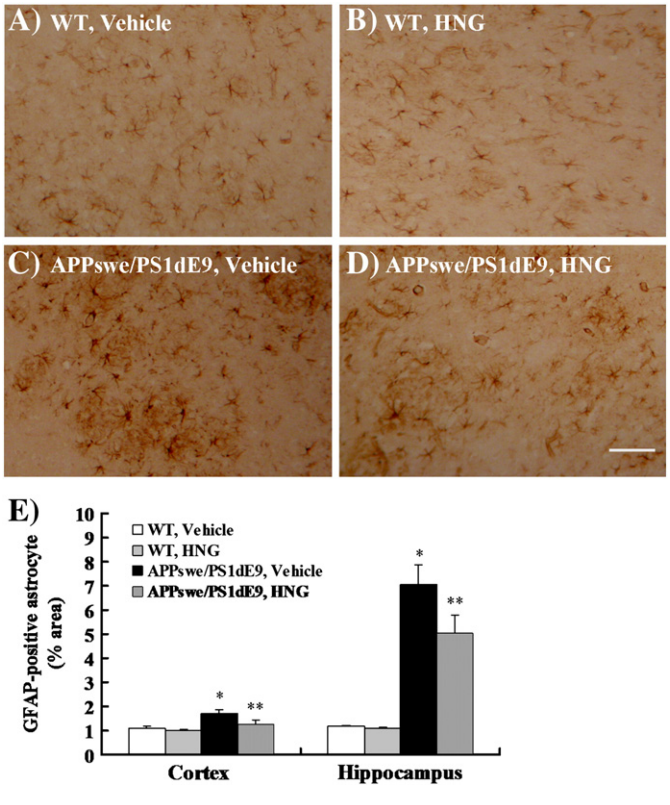

Fig. 5. HNG treatment reduced the amount of reactive astrocytes in APPswe/PS1dE9 mice. Representative immunostaining of GFAP-positive astrocytes in the frontal cortex of vehicle-treated WT mice (A), HNG-treated WT mice (B), vehicle-treated APPswe/PS1dE9 mice (C), and HNG-treated APPswe/PS1dE9 mice (D). Quantitative analysis disclosed that the amount of reactive astrocytes in cerebral cortex and hippocampus was significantly increased in vehicle-treated APPswe/PS1dE9 mice compared with vehicle- and HNG-treated WT mice (E), while HNG treatment in APPswe/PS1dE9 mice significantly reduced the amount of reactive astrocytes in cerebral cortex and hippocampus compared with vehicle-treated APPswe/PS1dE9 mice (E). No significant difference in the amount of reactive astrocytes in cerebral cortex and hippocampus was found between vehicle- and HNG-treated WT mice (E; $p>0.05$). Each value represents the mean ± SEM from 8 mice per group. $^{*}p<0.001$ versus vehicle- and HNG-treated WT mice; $^{**}p<0.01$ versus vehicle-treated APPswe/PS1dE9 mice. Scale bar = 100 μm.

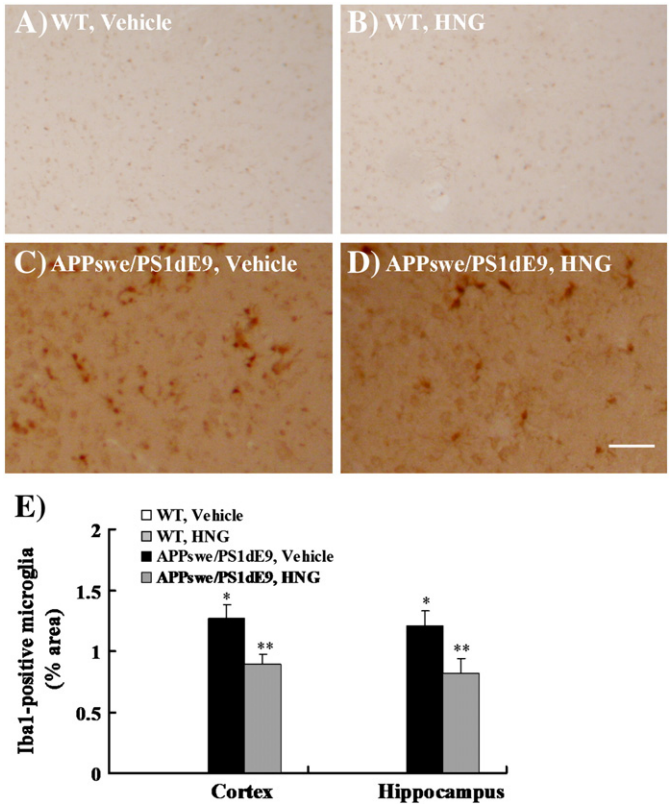

Fig. 6. HNG treatment reduced microglial activation in APPswe/PS1dE9 mice. Representative immunostaining of Iba1-positive microglia in the frontal cortex of vehicle-treated WT mice (A), HNG-treated WT mice (B), vehicle-treated APPswe/PS1dE9 mice (C), and HNG-treated APPswe/PS1dE9 mice (D). Quantitative analysis disclosed that the amount of activated microglia in cerebral cortex and hippocampus was significantly increased in vehicle-treated APPswe/PS1dE9 mice compared with vehicle- and HNG-treated WT mice (E), while HNG treatment in APPswe/PS1dE9 mice significantly reduced the amount of activated microglia in cerebral cortex and hippocampus compared with vehicle-treated APPswe/PS1dE9 mice (E). No significant difference in the amount of activated microglia in cerebral cortex and hippocampus was found between vehicle- and HNG-treated WT mice (E; $p>0.05$). Each value represents the mean ± SEM from 8 mice per group. $^{*}p<0.001$ versus vehicle- and HNG-treated WT mice; $^{**}p<0.01$ versus vehicle-treated APPswe/PS1dE9 mice. Scale bar = 100 μm.

by determining the concentration of insoluble Aβ peptides, showing a marked decrease in insoluble Aβ levels (e.g., total Aβ1-x, Aβ1-40, and Aβ1-42) in cerebral cortex and hippocampus in HNG-treated APPswe/PS1dE9 mice compared with vehicle-treated APPswe/PS1dE9 mice. Since the insoluble Aβ peptide is a major component of plaques, decreased insoluble Aβ levels are in line with the morphometric findings showing a reduced Aβ deposits, particularly fibrillar Aβ deposition, in HNG-treated APPswe/PS1dE9 mice. Combined with the ELISA and morphometric results, these data indicate that HNG may suppress the age-related increase of plaque burden and insoluble Aβ levels in APPswe/PS1dE9 mouse brains. This is consistent with the previous study showing that intranasal treatment of HNG may reduce the amount of amyloid plaques (stained with anti-Aβ antibody 82E1) in 3xTg-AD female mice (Niikura et al., 2011). However, we did not find significant difference in the levels of APP βCTF and soluble Aβ (e.g., total Aβ1-x, Aβ1-40, and Aβ1-42) between HNG- and vehicle-treated APPswe/PS1dE9 mice, suggesting that HNG treatment had little effect on APP processing and Aβ production, which is in agreement with the previous studies showing that HN and its derivatives (HNG) could not inhibit the production of Aβ from APP in vitro (Hashimoto et al., 2001; Jung and Van Nostrand, 2003) and in vivo (Niikura et al., 2011). Overall, these results indicate that HNG may have a clear beneficial effect on reducing some forms of Aβ burden in the brain.

Neuroinflammation has been documented to be a well-defined feature of AD pathology, which is believed to play an important role in the pathogenesis of AD (Di Bona et al., 2010). Previous study has shown that robust activated microglia and astrocytes as well as increased cytokines in APPswe/PS1dE9 mice as they age and Aβ-associated pathology progresses (Ruan et al., 2009). Quantitative analyses in the present study revealed that vehicle-treated APPswe/PS1dE9 mice had significantly elevated inflammatory responses (i.e., reactive astrocytes, activated microglia, IL-1β, IL-6, and TNFα) compared with vehicle- and HNG-treated WT mice, while HNG treatment in APPswe/PS1dE9 mice led to a significant reduction in astrocytic activation and microglial activation as well as several inflammatory cytokines' levels (i.e., IL-1β, IL-6, and TNFα) compared with vehicle-treated APPswe/PS1dE9 mice. Given the central role of fibrillar Aβ deposition in the activation of microglia and astrocytes seen in AD, and inflammatory cytokines produced primarily by these activated glia (Rozemuller et al., 2005; Hoozemans et al., 2006), the significant decrease in neuroinflammation seen in HNG-treated APPswe/PS1dE9 mice can be attributed to the lowering of the Aβ plaque burden, particularly the fibrillar Aβ plaques. In addition, this reduction in neuroinflammation, at least in part, may result from HNG's anti-inflammatory property, evidenced by HNG significantly decreasing neuroinflammatory responses (i.e., reactive astrocytes, activated microglia, IL-6, and TNFα) in Aβ-infused mice (Miao et al., 2008). Together, these results indicate that HNG can reduce the Aβ-associated neuroinflammation.

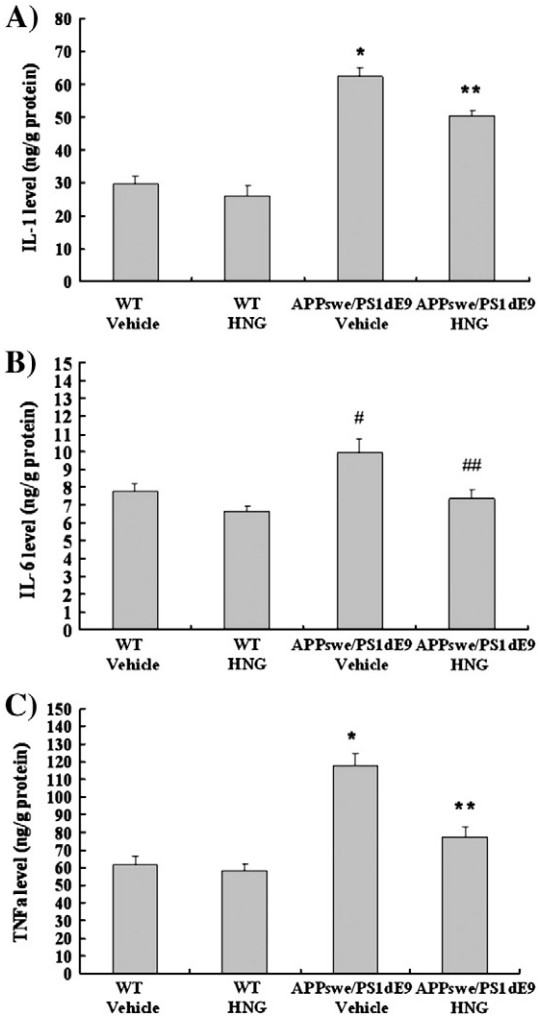

Fig. 7. HNG treatment reduced inflammatory cytokine levels in APPswe/PS1dE9 mice. Quantitative analysis disclosed that the levels of IL-1β (A), IL-6 (B), and TNFα (C) were significantly elevated in vehicle-treated APPswe/PS1dE9 mice compared with vehicle- and HNG-treated WT mice, while HNG treatment in APPswe/PS1dE9 mice significantly reduced the levels of IL-1β (A), IL-6 (B), and TNFα (C) compared with vehicle-treated APPswe/PS1dE9 mice. No significant differences in the levels of these cytokines were observed between vehicle- and HNG-treated WT mice ($p>0.05$). Each value represents the mean ± SEM from 8 mice per group. $^{*}p<0.001$, $^{\#}p<0.01$ versus vehicle- and HNG-treated WT mice; $^{**}p<0.001$, $^{\#\#}p<0.01$ versus vehicle-treated APPswe/PS1dE9 mice.

In addition, no significant differences in the behavioral performance and neuroinflammatory responses were found between vehicle- and HNG-treated WT mice, indicating that HNG itself could not directly enhance or impair cognitive function, and evoke an increase of neuroinflammation in the brain, which is consistent with our previous findings (Miao et al., 2008). Therefore, the beneficial effect of HNG treatment on the improvement of spatial learning and memory deficits in APPswe/PS1dE9 mice may be attributable to its combined effects on reducing some forms of Aβ burden and its related neuroinflammation. Further studies are required to clarify the underlying mechanisms by which HNG might significantly reduce the Aβ-related neuropathology and benefit the cognitive decline in established AD.

In summary, the present results provide evidence that chronic HNG treatment may improve cognitive deficits and reduce Aβ burden and neuroinflammation in the middle-aged APPswe/PS1dE9 mice with pre-existing abundant Aβ pathology, suggesting that HNG may have therapeutic potential in the treatment of AD even with large amounts of Aβ-associated pathology.

Supplementary materials related to this article can be found online at doi: 10.1016/j.pbb.2011.09.012.

Acknowledgments

This work was financially supported by the research grants from the National Natural Science Foundation of China (30870842; 30801215). We are very grateful to Dr. Changsheng Chen (Department of Medical Statistics, Fourth Military Medical University) for his expert technical assistance in statistical analyses.

References

Arakawa T, Kita Y, Niikura T. A rescue factor for Alzheimer's diseases: discovery, activity, structure, and mechanism. Curr Med Chem 2008;15:2086–98.
Blurton-Jones M, Kitazawa M, Martinez-Coria H, Castello NA, Müller FJ, Loring JF, et al. Neural stem cells improve cognition via BDNF in a transgenic model of Alzheimer disease. Proc Natl Acad Sci USA 2009;106:13594–9.
Butovsky O, Koronyo-Hamaoui M, Kunis G, Ophir E, Landa G, Cohen H, et al. Glatiramer acetate fights against Alzheimer's disease by inducing dendritic-like microglia expressing insulin-like growth factor 1. Proc Natl Acad Sci USA 2006;103:11784–9.
Cappell J, Herrmann N, Cornish S, Lanctôt KL. The pharmacoeconomics of cognitive enhancers in moderate to severe Alzheimer's disease. CNS Drugs 2010;24:909–27.
Di Bona D, Scapagnini G, Candore G, Castiglia L, Colonna-Romano G, Duro G, et al. Immune-inflammatory responses and oxidative stress in Alzheimer's disease: therapeutic implications. Curr Pharm Des 2010;16:684–91.
Edbauer D, Winkler E, Regula JT, Pesold B, Steiner H, Haass C. Reconstitution of gamma-secretase activity. Nat Cell Biol 2003;5:486–8.
Fan R, Xu F, Previti ML, Davis J, Grande AM, Robinson JK, et al. Minocycline reduces microglial activation and improves behavioral deficits in a transgenic model of cerebral microvascular amyloid. J Neurosci 2007;27:3057–63.
Garcia-Alloza M, Robbins EM, Zhang-Nunes SX, Purcell SM, Betensky RA, Raju S, et al. Characterization of amyloid deposition in the APPswe/PS1dE9 mouse model of Alzheimer disease. Neurobiol Dis 2006;24:516–24.
Hardy J, Selkoe DJ. The amyloid hypothesis of Alzheimer's disease: progress and problems on the road to therapeutics. Science 2002;297:353–6.
Hashimoto Y, Niikura T, Tajima H, Yasukawa T, Sudo H, Ito Y, et al. A rescue factor abolishing neuronal cell death by a wide spectrum of familial Alzheimer's disease genes and Abeta. Proc Natl Acad Sci USA 2001;98:6336–41.
Herrmann N, Li A, Lanctôt K. Memantine in dementia: a review of the current evidence. Expert Opin Pharmacother 2011;12:787–800.
Hoozemans JJ, Veerhuis R, Rozemuller JM, Eikelenboom P. Neuroinflammation and regeneration in the early stages of Alzheimer's disease pathology. Int J Dev Neurosci 2006;24:157–65.
Imbimbo BP, Giardino L, Sivilia S, Giuliani A, Gusciglio M, Pietrini V, et al. CHF5074, a novel gamma-secretase modulator, restores hippocampal neurogenesis potential and reverses contextual memory deficit in a transgenic mouse model of Alzheimer's disease. J Alzheimers Dis 2010;20:159–73.
Jin H, Liu T, Wang WX, Xu JH, Yang PB, Lu HX, et al. Protective effects of [Gly14]-Humanin on beta-amyloid-induced PC12 cell death by preventing mitochondrial dysfunction. Neurochem Int 2010;56:417–23.
Jung SS, Van Nostrand WE. Humanin rescues human cerebrovascular smooth muscle cells from Abeta-induced toxicity. J Neurochem 2003;84:266–72.
Kemppainen NM, Aalto S, Wilson IA, Någren K, Helin S, Brück A, et al. PET amyloid ligand [11C]PIB uptake is increased in mild cognitive impairment. Neurology 2007;68:1603–6.
Krejcova G, Patocka J, Slaninova J. Effect of humanin analogues on experimentally induced impairment of spatial memory in rats. J Pept Sci 2004;10:636–9.
Kunesová G, Hlavácek J, Patocka J, Evangelou A, Zikos C, Benaki D, et al. The multiple T-maze in vivo testing of the neuroprotective effect of humanin analogues. Peptides 2008;29:1982–7.
Lalonde R, Kim HD, Maxwell JA, Fukuchi K. Exploratory activity and spatial learning in 12-month-old APP(695)SWE/co + PS1/DeltaE9 mice with amyloid plaques. Neurosci Lett 2005;390:87–92.
Li N, Liu GT. The novel squamosamide derivative FLZ enhances BDNF/TrkB/CREB signaling and inhibits neuronal apoptosis in APP/PS1 mice. Acta Pharmacol Sin 2010;31:265–72.
Lleó A, Greenberg SM, Growdon JH. Current pharmacotherapy for Alzheimer's disease. Annu Rev Med 2006;57:513–33.
Mamiya T, Ukai M. [Gly(14)]-Humanin improved the learning and memory impairment induced by scopolamine in vivo. Br J Pharmacol 2001;134:1597–9.
Maurice T, Hippert C, Serratrice N, Dubois G, Jacquet C, Antignac C, et al. Cystine accumulation in the CNS results in severe age-related memory deficits. Neurobiol Aging 2009;30:987-1000.
Miao J, Vitek MP, Xu F, Previti ML, Davis J, Van Nostrand WE. Reducing cerebral microvascular amyloid-beta protein deposition diminishes regional neuroinflammation in vasculotropic mutant amyloid precursor protein transgenic mice. J Neurosci 2005;25:6271–7.
Miao J, Zhang W, Yin R, Liu R, Su C, Lei G, et al. S14G-Humanin ameliorates Abeta25-35-induced behavioral deficits by reducing neuroinflammatory responses and apoptosis in mice. Neuropeptides 2008;42:557–67.
Minkeviciene R, Banerjee P, Tanila H. Memantine improves spatial learning in a transgenic mouse model of Alzheimer's disease. J Pharmacol Exp Ther 2004;311:677–82.
Minkeviciene R, Ihalainen J, Malm T, Matilainen O, Keksa-Goldsteine V, Goldsteins G, et al. Age-related decrease in stimulated glutamate release and vesicular glutamate

transporters in APP/PS1 transgenic and wild-type mice. J Neurochem 2008;105: 584–94.
Mori T, Town T, Tan J, Yada N, Horikoshi Y, Yamamoto J, et al. Arundic Acid ameliorates cerebral amyloidosis and gliosis in Alzheimer transgenic mice. J Pharmacol Exp Ther 2006;318:571–8.
Niikura T, Sidahmed E, Hirata-Fukae C, Aisen PS, Matsuoka Y. A humanin derivative reduces amyloid Beta accumulation and ameliorates memory deficit in triple transgenic mice. PLoS One 2011;6:e16259.
Niikura T, Tajima H, Kita Y. Neuronal cell death in Alzheimer's disease and a neuroprotective factor, humanin. Curr Neuropharmacol 2006;4:139–47.
Nishimoto I, Matsuoka M, Niikura T. Unravelling the role of Humanin. Trends Mol Med 2004;10:102–5.
O'Hare E, Scopes DI, Treherne JM, Norwood K, Spanswick D, Kim EM. RS-0406 arrests amyloid-beta oligomer-induced behavioural deterioration in vivo. Behav Brain Res 2010;210:32–7.
Oksman M, Iivonen H, Hogyes E, Amtul Z, Penke B, Leenders I, et al. Impact of different saturated fatty acid, polyunsaturated fatty acid and cholesterol containing diets on beta-amyloid accumulation in APP/PS1 transgenic mice. Neurobiol Dis 2006;23: 563–72.
O'Leary TP, Brown RE. Visuo-spatial learning and memory deficits on the Barnes maze in the 16-month-old APPswe/PS1dE9 mouse model of Alzheimer's disease. Behav Brain Res 2009;201:120–7.
Peng Y, Sun J, Hon S, Nylander AN, Xia W, Feng Y, et al. L-3-n-butylphthalide improves cognitive impairment and reduces amyloid-beta in a transgenic model of Alzheimer's disease. J Neurosci 2010;30:8180–9.
Rozemuller AJ, van Gool WA, Eikelenboom P. The neuroinflammatory response in plaques and amyloid angiopathy in Alzheimer's disease: therapeutic implications. Curr Drug Targets CNS Neurol Disord 2005;4:223–33.
Ruan L, Kang Z, Pei G, Le Y. Amyloid deposition and inflammation in APPswe/PS1dE9 mouse model of Alzheimer's disease. Curr Alzheimer Res 2009;6:531–40.
Savonenko A, Xu GM, Melnikova T, Morton JL, Gonzales V, Wong MP, et al. Episodic-like memory deficits in the APPswe/PS1dE9 mouse model of Alzheimer's disease: relationships to beta-amyloid deposition and neurotransmitter abnormalities. Neurobiol Dis 2005;18:602–17.
Schenk D. Current challenges for the successful treatment and prevention of Alzheimer's disease: treating the pathologies of the disease to change its clinical course. Alzheimers Dement 2008;4:S119–21.
Selkoe DJ. Alzheimer's disease: genes, proteins, and therapy. Physiol Rev 2001;81: 741–66.
Selkoe DJ. Cell biology of the amyloid beta-protein precursor and the mechanism of Alzheimer's disease. Annu Rev Cell Biol 1994;10:373–403.
Seltzer B. Cholinesterase inhibitors in the clinical management of Alzheimer's disease: importance of early and persistent treatment. J Int Med Res 2006;34:339–47.
Smith M, Wells J, Borrie M. Treatment effect size of memantine therapy in Alzheimer disease and vascular dementia. Alzheimer Dis Assoc Disord 2006;20:133–7.
St George-Hyslop PH, Petit A. Molecular biology and genetics of Alzheimer's disease. C R Biol 2005;328:119–30.
Tajima H, Kawasumi M, Chiba T, Yamada M, Yamashita K, Nawa M, et al. A humanin derivative, S14G-HN, prevents amyloid-beta-induced memory impairment in mice. J Neurosci Res 2005;79:714–23.
Van Marum RJ. Current and future therapy in Alzheimer's disease. Fundam Clin Pharmacol 2008;22:265–74.
Wang H, Liu J, Zong Y, Xu Y, Deng W, Zhu H, et al. miR-106b aberrantly expressed in a double transgenic mouse model for Alzheimer's disease targets TGF-β type II receptor. Brain Res 2010;1357:166–74.
Wang X, Liu P, Zhu H, Xu Y, Ma C, Dai X, et al. miR-34a, a microRNA up-regulated in a double transgenic mouse model of Alzheimer's disease, inhibits bcl2 translation. Brain Res Bull 2009;80:268–73.
Xu X, Chua CC, Gao J, Hamdy RC, Chua BH. Humanin is a novel neuroprotective agent against stroke. Stroke 2006;37:2613–9.
Yamakawa H, Yagishita S, Futai E, Ishiura S. beta-Secretase inhibitor potency is decreased by aberrant beta-cleavage location of the "Swedish mutant" amyloid precursor protein. J Biol Chem 2010;285:1634–42.
Zhang L, Xing Y, Ye CF, Ai HX, Wei HF, Li L. Learning-memory deficit with aging in APP transgenic mice of Alzheimer's disease and intervention by using tetrahydroxystilbene glucoside. Behav Brain Res 2006;173:246–54.
Zhang W, Hao J, Liu R, Zhang Z, Lei G, Su C, et al. Soluble Aβ levels correlate with cognitive deficits in the 12-month-old APPswe/PS1dE9 mouse model of Alzheimer's disease. Behav Brain Res 2011;222:342–50.